



Dugdale, S. B. (2011). First-principles study of electron-phonon superconductivity in YSn_3 . *Physical Review B: Condensed Matter and Materials Physics*, 83(1), 1-4. [012502].
<https://doi.org/10.1103/PhysRevB.83.012502>

Publisher's PDF, also known as Version of record

Link to published version (if available):
[10.1103/PhysRevB.83.012502](https://doi.org/10.1103/PhysRevB.83.012502)

[Link to publication record in Explore Bristol Research](#)
PDF-document

University of Bristol - Explore Bristol Research

General rights

This document is made available in accordance with publisher policies. Please cite only the published version using the reference above. Full terms of use are available:
<http://www.bristol.ac.uk/red/research-policy/pure/user-guides/ebr-terms/>

First-principles study of electron-phonon superconductivity in YSn₃

S. B. Dugdale

H. H. Wills Physics Laboratory, University of Bristol, Tyndall Avenue, Bristol BS8 1TL, United Kingdom

(Received 12 October 2010; published 10 January 2011)

First-principles calculations of the cubic intermetallic compound YSn₃ indicate that the superconductivity it exhibits below 7 K can be explained by intermediate strength conventional electron-phonon coupling. With a reasonable value for the Coulomb pseudopotential $\mu^* = 0.12$, and the calculated electron-phonon coupling constant of 0.99, the McMillan formula predicts a T_c of approximately 6 K.

DOI: [10.1103/PhysRevB.83.012502](https://doi.org/10.1103/PhysRevB.83.012502)

PACS number(s): 74.25.Jb, 71.38.-k, 74.25.Kc

Light rare-earth trisnannides have been found to play host to a wide variety of phenomena. Exhibiting the AuCu₃ structure with the space group $Pm\bar{3}m$ (number 221, see Fig. 1), some possess antiferromagnetic ground states (PrSn₃ and NdSn₃),¹ PrSn₃ exhibits heavy fermion behavior,² and LaSn₃ superconducts at about 6.25 K.³ However, synthesis of the heavier rare-earth compounds (and also YSn₃) demanded high-pressure and high-temperature methods,⁴ and the compounds produced were apt to decompose to metallic tin within a couple of weeks of being exposed to air. High-pressure synthesis has recently been successful in producing polycrystalline samples of YSn₃, in which superconductivity was subsequently found ($T_c = 7$ K).⁵ The normalized jump in the specific heat ($\frac{\Delta C}{\gamma T_c}$, where γ is the Sommerfeld coefficient) was found to be 2.19, larger than the weak-coupling BCS value of 1.43. Previously, there have been a number of studies on the band structure of LaSn₃,^{6–8} but no calculations are reported for YSn₃. Understanding the origin of the superconductivity is the motivation for the study presented here. In this Brief Report, *ab initio* calculations are used to show that this superconductivity can be explained by intermediate strength electron-phonon coupling.

Two separate sets of calculations were performed, the first using the highly accurate all-electron full-potential linearized augmented plane-wave method (often referred to as FP-LAPW), as implemented in the ELK code,⁹ and the second using pseudopotentials, as implemented within the QUANTUM ESPRESSO code,¹⁰ for the calculation of the phonons and electron-phonon coupling. The lattice constant was fixed at the experimental one ($a = 4.667$ Å), and calculations were made using the ELK code⁹ with a cutoff (for plane waves in the interstitial region) determined by $k_{\max} = 9.0/R_{\min}$, where R_{\min} is the smallest muffin-tin radius. The muffin-tin radii for Y and Sn were 2.85 a.u. and 2.96 a.u., respectively. Convergence was obtained on a mesh of 816 k points in the irreducible Brillouin zone. The initial calculations neglected spin-orbit coupling, and the Perdew-Burke-Ernzerhof generalized gradient approximation (GGA) exchange-correlation functional was used.¹¹ The resulting band structure and density of states (DOS) are shown in Figs. 2 and 3, respectively. The lowest manifold comprises Sn s states, while those at the Fermi level are predominantly of Sn p character with a slight degree of hybridization with Y d .

The DOS at the Fermi energy, $N(E_F)$, can be related to the Sommerfeld coefficient γ that appears in the expression for

the electronic contribution to the specific heat,

$$C_{el} = \gamma T = \frac{\pi^2}{3} k_B^2 N(E_F) T. \quad (1)$$

The experimentally determined γ^{exp} can be considered to be renormalized by many-body effects, which are not included in the calculation. Assuming that the electron-phonon interaction is the dominant many-body effect (and explicitly neglecting the others), the renormalization permits the evaluation of the electron-phonon coupling constant, λ_{ep} , through the relationship,

$$\frac{\gamma^{\text{exp}}}{\gamma^{\text{calc}}} = 1 + \lambda_{ep}. \quad (2)$$

Using the calculated $N(E_F)$ of 1.92 states (eV cell)^{−1}, γ^{calc} is 4.53 mJ/mol K², and by taking γ^{exp} extracted by Kawashima *et al.* of 7.57 mJ/mol K²,⁵ an estimate for λ_{ep} of 0.63 can be obtained.

Returning to the band structure, three bands cross the Fermi level and the Fermi surfaces are shown in Fig. 4. Two sheets have simple topologies, but the third sheet has a rather complicated topology. In order to check that the inclusion of spin-orbit coupling (SOC) did not substantially alter the electronic structure (and in particular, the Fermi surface topology), a further self-consistent calculation was made in which a term $\sigma \cdot \mathbf{L}$ was added to the second-variational Hamiltonian.⁹ A comparison of the band structures computed both with and without SOC is made in Fig. 5. It can be seen that the effect of introducing SOC is very small, lifting some degeneracies in the band structure (for example, along Γ -X), but not radically changing the Fermi surface topology. Quantitatively, the inclusion of SOC reduces $N(E_F)$ by just over 1%, and therefore the neglect of it is unlikely to have a substantial impact on λ_{ep} . Finally, a comparison between the band structures of LaSn₃ and YSn₃, both including spin-orbit coupling, is shown in Fig. 6. As expected, the dispersions in the two compounds are very similar, but some small differences can be seen (for example, along Γ -X). For the LaSn₃ calculation, which is in agreement with earlier work,⁸ the presence of the 4*f* bands above the Fermi energy does not appear to have a strong effect on the dispersions of the bands at the Fermi energy.

To fully investigate electron-phonon superconductivity in YSn₃, the QUANTUM ESPRESSO package was used to calculate, by linear response, the phonon dispersions and the

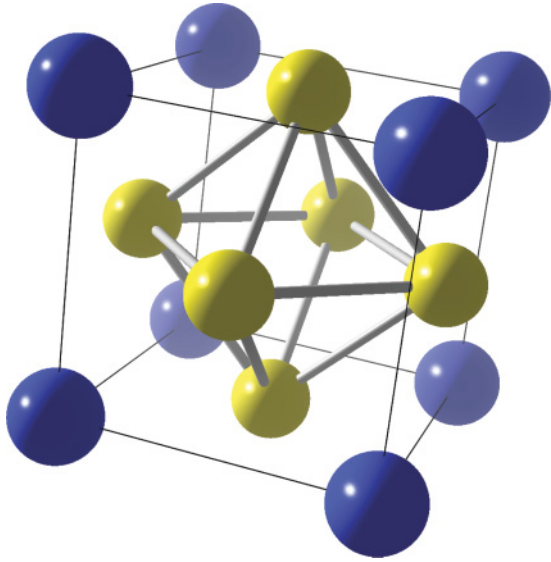


FIG. 1. (Color online) YSn_3 has the AuCu_3 structure with the space group $Pm\bar{3}m$. The Y atoms occupy the corners and the Sn atoms are at the face-centered positions.

electron-phonon coupling.¹⁰ Scalar relativistic ultrasoft pseudopotentials with the Perdew-Wang-91 GGA exchange-correlation functional¹² were chosen, and convergence was checked with respect to the k -point density and the plane-wave cutoffs, and subsequent calculations were made with wavefunction and charge-density cutoffs of 40 and 400 Ry, respectively. The computed band structure was barely distinguishable from that calculated by the all-electron FP-LAPW ELK code. Phonons were calculated on an $8 \times 8 \times 8$ Monkhorst-Pack q -point grid with Brillouin zone integrations on a $16 \times 16 \times 16$ mesh, while the electron-phonon coupling was evaluated with Brillouin zone integrations performed on a denser ($32 \times 32 \times 32$) mesh. The calculated phonon dispersion is shown in Fig. 7, and there are hints of strong electron-phonon interactions appearing as possible Kohn anomalies¹³ in the lowest acoustic phonon branch (for example, the apparent softening

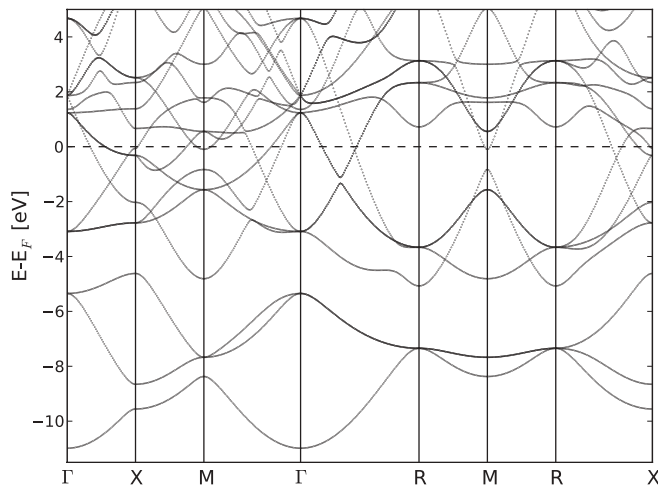


FIG. 2. Band structure of YSn_3 along selected high-symmetry directions.

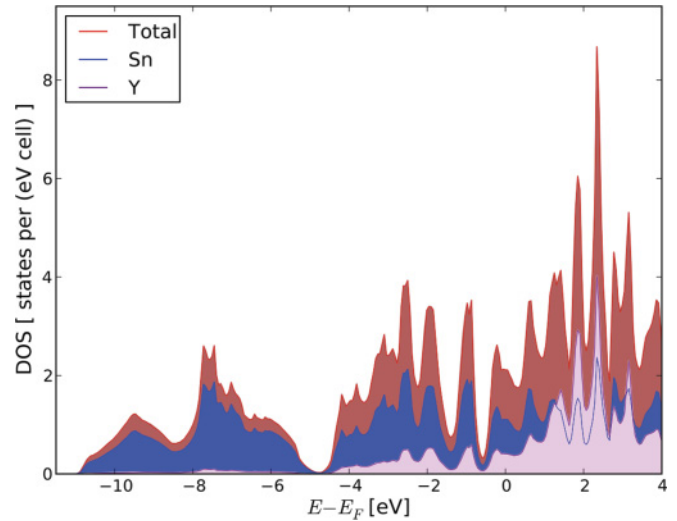


FIG. 3. (Color online) Density of states for YSn_3 , showing the total DOS in red (upper curve), the site-projected Sn DOS in blue (darkest shading) and Y DOS in lilac (lightest shading). The interstitial DOS is not plotted.

along Γ -R). There are, however, no imaginary frequencies that would explain the structural instabilities found in the material.

The phonon DOS $[F(\omega)]$ and the Eliashberg function $[\alpha^2 F(\omega)]$ are shown in Fig. 8. The strong resemblance between the shapes of the $\alpha^2 F(\omega)$ and $F(\omega)$ distributions suggests that the electron-phonon interaction does not vary greatly across the twelve phonon modes, and the calculations of the electron-phonon coupling constant λ_{ep} support this assertion. The total electron-phonon coupling constant λ_{ep} is found to be 0.99, meaning that the average λ_{ep} across each of the twelve phonon modes is 0.082. The contributions from the first three modes do, however, substantially exceed this average (0.22, 0.16, and 0.12, respectively), and this fact is responsible for the lowest peak in $\alpha^2 F(\omega)$ just above 1 THz. It is also in this energy range that the lowest acoustic phonon branch along Γ -R shows softening. The three acoustic modes have almost equal contributions from Sn and Y, but Sn atoms dominate the modes in the range 80–120 cm^{-1} . Above 120 cm^{-1} , both Y and Sn atoms contribute approximately equally once again.

Having calculated the relevant electron and phonon quantities, it is possible to estimate the superconducting critical temperature. For values of λ_{ep} that are less than 1.5, the McMillan formula can be used in place of the Allen-Dynes formula.^{14,15} Here,

$$T_c = \frac{\hbar\omega_{\text{ln}}}{1.2k_B} \exp\left(-\frac{1.04(1+\lambda_{ep})}{\lambda_{ep} - \mu^*(1+0.62\lambda_{ep})}\right), \quad (3)$$

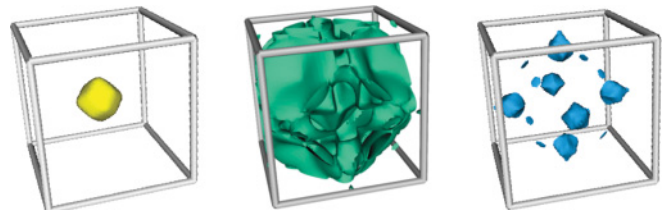


FIG. 4. (Color online) The three Fermi surface sheets of YSn_3 .

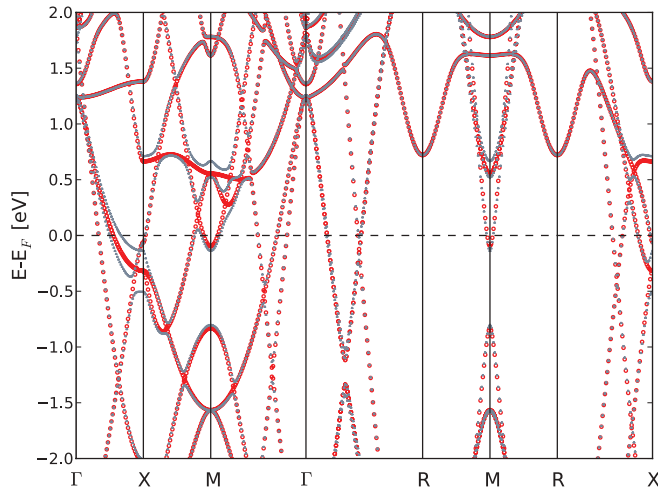


FIG. 5. (Color online) Detail of the band structure close to the Fermi energy, showing the small differences between the calculations with (small gray triangles) and without (open red circles) spin-orbit coupling.

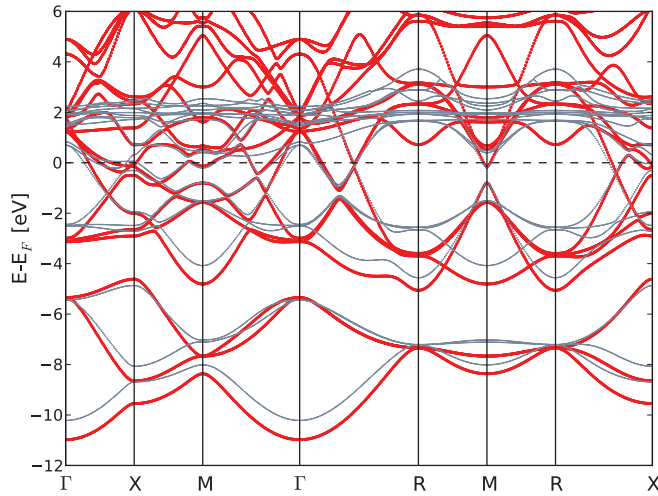


FIG. 6. (Color online) Comparison of the band structures of YSn_3 (thick red) and LaSn_3 (thin gray), both including SOC, along selected high-symmetry directions.

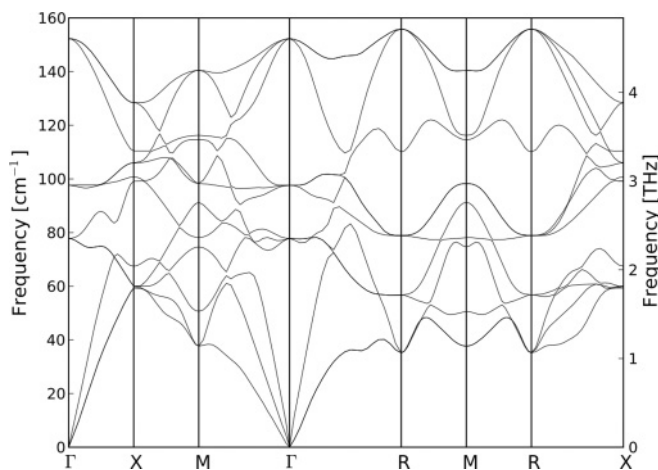


FIG. 7. Phonon dispersion along high-symmetry directions.

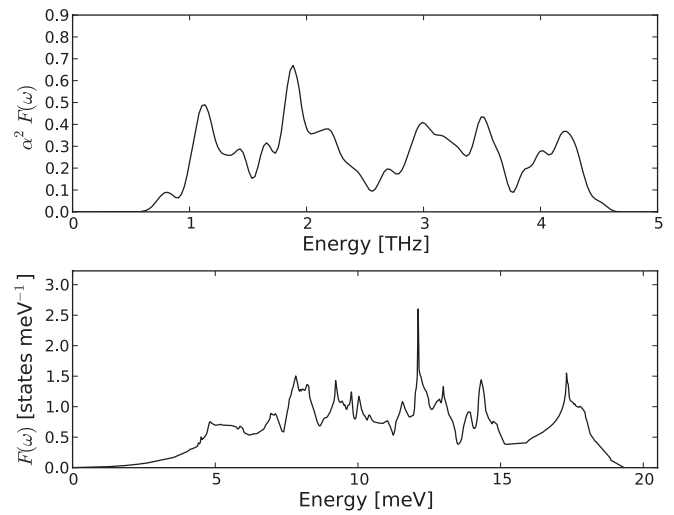


FIG. 8. Phonon DOS (bottom) and the Eliashberg function [$\alpha^2 F(\omega)$]. As 1 THz is equivalent to 4.1 meV (or 33 cm^{-1}), the ranges spanned by the two separate plots are equivalent.

where λ_{ep} is the electron-phonon coupling, ω_{\ln} is the logarithmically averaged phonon frequency, and the dimensionless μ^* is the Coulomb pseudopotential, which characterizes the strength of the (screened) electron-electron Coulomb repulsion. From the calculations, by taking $\lambda_{ep} = 0.99$, $\omega_{\ln} = 65 \text{ cm}^{-1}$, and $\mu^* = 0.12$ (a typical choice, but values between 0.10 and 0.15 are reasonable), a T_c of 5.93 K is obtained. This is in rather good agreement with the experimentally observed value of 7 K.⁵ In LaSn_3 , which has a very similar T_c of 6.25 K,³ de Haas–van Alphen measurements reported enhancement of cyclotron masses compatible with a λ_{ep} of about one,⁸ and a similar conclusion about the size of λ_{ep} in LaSn_3 was reached after the kind of analysis of the specific heat presented earlier in this paper.⁶ The consistency in these two estimated values for λ_{ep} in LaSn_3 and its similar T_c to YSn_3 suggests that the estimate for λ_{ep} presented earlier, based on electronic specific heat data, should probably be trusted much less than the fully *ab initio* approach, particularly given the challenging nature of the experiment, which may have been complicated by the presence of a Sn impurity phase.⁵

In conclusion, an *ab initio* study of the electronic and phononic structure of YSn_3 has been conducted in order to understand the origin of superconductivity in YSn_3 . The calculations make predictions about physical properties that can be obtained from the electronic band structure and the phonon dispersions. These indicate that the strength of the electron-phonon coupling λ_{ep} is 0.99, which, together with the computed logarithmically averaged phonon frequency, gives (via the McMillan equation) a T_c of about 6 K, which is in good agreement with experiment. The physical relevance of this study is, therefore, that the superconductivity can be accounted for by the conventional electron-phonon interaction, in the intermediate coupling regime.

This work was carried out using the computational facilities of the Advanced Computing Research Centre, University of Bristol [<http://www.bris.ac.uk/acrc/>].

- ¹G. K. Shenoy, B. D. Dunlap, G. M. Kalvius, A. M. Toxen, and R. J. Gambino, *J. Appl. Phys.* **41**, 1317 (1970).
- ²R. Settai, K. Sugiyama, A. Yamaguchi, S. Araki, K. Miyake, T. Takeuchi, K. Kindo, Y. Onuki, and Z. Kletowski, *J. Phys. Soc. Jpn.* **69**, 3983 (2000).
- ³R. J. Gambino, N. R. Stemple, and A. M. Toxen, *J. Phys. Chem. Solids* **29**, 295 (1968).
- ⁴K. Miller and H. T. Hall, *Inorg. Chem.* **11**, 1188 (1972).
- ⁵K. Kawashima, M. Maruyama, M. Fukuma, and J. Akimitsu, *Phys. Rev. B* **82**, 094517 (2010).
- ⁶A. Hasegawa, *J. Phys. Soc. Jpn.* **50**, 3313 (1981).
- ⁷R. M. Boulet, J. P. Jan, and H. L. Skriver, *J. Phys. F* **12**, 293 (1982).
- ⁸A. Hasegawa and H. Yamagami, *J. Phys. Soc. Jpn.* **60**, 1654 (1991).
- ⁹See [<http://elk.sourceforge.net>]
- ¹⁰P. Gianozzi *et al.*, *J. Phys.: Condens. Matter* **21**, 395502 (2009); see also [<http://www.quantum-espresso.org>]
- ¹¹J. P. Perdew, K. Burke, and M. Ernzerhof, *Phys. Rev. Lett.* **77**, 3865 (1996).
- ¹²J. P. Perdew, in *Electronic Structure of Solids 91*, edited by P. Ziesche and H. Eschrig (Akademie Verlag, Berlin, 1991), p. 11.
- ¹³W. Kohn, *Phys. Rev. Lett.* **2**, 393 (1959).
- ¹⁴P. B. Allen and R. C. Dynes, *J. Phys. C* **8**, L158 (1975).
- ¹⁵W. L. McMillan, *Phys. Rev.* **167**, 331 (1968).